

Vibrational Spectra and 266 nm Photochemistry of ClNO₂ Thin Films and ClNO₂ in Amorphous Water Ice

L. Schriver-Mazzuoli,^{*,†,‡} A. Schriver,[†] J. M. Coanga,[†] and M. Steers[‡]

Laboratoire de Physique Moléculaire et Applications,[§] UMR 7092, Université Pierre et Marie Curie, Tour 13, case 76, 4 place Jussieu, 75252 Paris Cedex 05, France, and Laboratoire d'Etude des Nuisances Atmosphériques et de leurs Effets, Université Paris-Nord, Campus de Bobigny, IUP Ville et Santé, Rue de la Convention, Bobigny 93017

Received: May 31, 2002; In Final Form: October 17, 2002

FTIR spectra of solid ClNO₂ in interaction or not with amorphous water ice between 11 and 200 K were analyzed, and the photochemistry of these solids was investigated. When ClNO₂ is deposited on an ice surface at 30 K or trapped in the water lattice, no ionization or reaction with water is observed even after annealing from 30 to 180 K. Photolysis of thin ClNO₂ films at 266 nm produced dinitrogen tetra-oxide as primary product. When ClNO₂ is trapped in ice, exposure to ultraviolet light quantitatively converted ClNO₂ to nitric acid hydrates.

Introduction

UV absorption of gaseous ClNO₂ exhibits a weak, regular vibronic structure superimposed on a broad unstructured background in the range 100–380 nm.¹ At 248 nm, only the formation of the primary fragments Cl + NO₂ was found active.^{1,2} Recently, the photodissociation at 266 nm of ClNO₂ in argon, oxygen, and nitrogen matrixes were investigated in our group.³ Significant differences between gas and condensed matrix photochemistry have been found. In matrixes, formation of ClONO (cis and trans) in equilibrium with ClNO₂ is observed after irradiation at 266 nm. On prolonged photolysis, ClONO dissociates into ClON and O and into ClO and NO. In an argon matrix, because of cage recombination, ClO and NO are not observed at all. In a nitrogen matrix, recombination of NO and NO₂ leads to N₂O₃ and secondary nitrogen oxide products.¹² As a continuation of these studies on the dependence of the photochemistry on the surrounding environment, the goal of this present work was to investigate, for the first time, the photochemistry at 266 nm of pure nitryl chloride (ClNO₂) in ClNO₂ or in amorphous ice films deposited on a cold gold surface under ultrahigh vacuum. Photoproducts were monitored by FTIR spectroscopy. In the troposphere, nitryl chloride can be formed by the reaction of gaseous N₂O₅ with NaCl salt aerosol.^{4,5} Under stratospheric conditions, ClNO₂ is possibly formed via the reaction of N₂O₅ with HCl dissolved in ice particles of polar stratospheric clouds.⁶ Nitryl chloride can also originate from isomerization of the cis isomer ClONO formed in the gas phase by reaction between atomic chlorine and NO₂⁷ or between Cl₂O and ClNO.⁸

Previous to photochemistry study, vibrational spectra of neat solid ClNO₂ were reinvestigated, and the sublimation energy of ClNO₂ has been determined. The interaction of nitryl chloride with a water ice surface was also examined on two types of ices: amorphous ice deposited from water vapor at 30 K and crystalline ice deposited from vapor at 160 K and then cooled

at 30 K. Finally, infrared spectra of mixed films containing amorphous ice in excess and ClNO₂ were reported with attention to temperature effects between 10 and 170 K. As a part of their study of the heterogeneous reaction between dinitrogen pentoxide and chlorine ions on low-temperature thin films, Sodeau et al.⁹ reported that co-depositing ClNO₂ with water at 80 K led to the formation of amorphous D_{2h} N₂O₄ with a trace of cis ClONO molecule. Our results do not support this observation. No surface processes leading to the formation of secondary products from reactions between ClNO₂ and water ice have been evidenced.

The results are presented in two parts. The first part is devoted to the spectroscopic studies and the second part to the photochemistry studies.

Experimental Section

ClNO₂ was synthesized by the reaction of an excess of ozone with nitrosyl chloride (ClNO) at room temperature.¹⁰ Ozone was prepared by silent electrical discharge through oxygen in a closed system cooled with liquid nitrogen using O₂ (N 45 from Air Liquide). ClNO from Merck Schuhardt was condensed at 77 K and subjected to several freeze–pump–thaw cycles before being mixed with ozone. After reaction of O₃ with ClNO, residual oxygen was removed by pumping on the condensate kept at 90 K followed by purification of ClNO₂ by trap-to-trap distillation at 200 K. The product was stored in the dark at liquid nitrogen temperature until needed. No impurities as NO₂, ClNO, and H₂O were observed in the IR spectra.

The experiments were performed using a closed cycle helium refrigerator (Air Product, Displex 202 A), which was pumped continuously (10⁻⁷ mbar background pressure range) and equipped with a rotatable sample holder. Thin films of ice or of ClNO₂ or of H₂O–ClNO₂ mixtures were supported inside upon a thermostated gold side of a substrate cube. The temperature of the metal substrate (11–200 K) was controlled by a silicon diode (Scientific Instruments 9600-1). Water was de-ionized, triply distilled, and then degassed by freeze–thaw cycles under vacuum before use. Pure water layers were grown from water vapor via a capillary connected to a pulsed dosing

* To whom correspondence should be addressed.

† Université Pierre et Marie Curie.

‡ Université Paris-Nord.

§ Laboratoire Associé à l'Université P. et M. Curie.

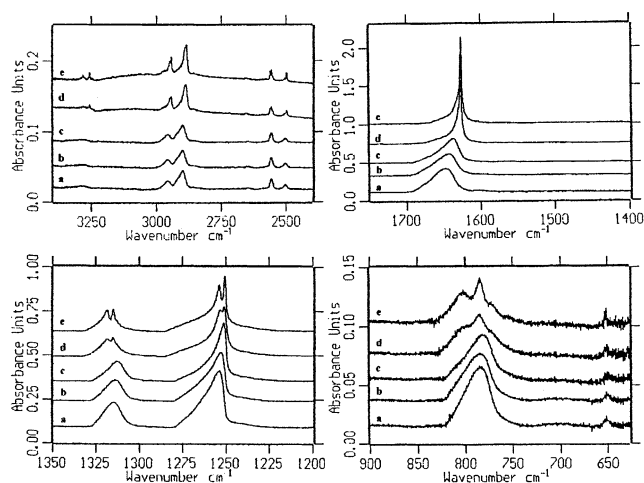


Figure 1. Vibrational spectrum of solid ClNO_2 recorded at (a) 30, (b) 50, (c) 70, (d) 80, and (e) 90 K.

system, which provides 2 ms long pulses of gas at a frequency of one pulse per 2 s. ClNO_2 films or mixed water/ ClNO_2 films were condensed at 30 K with helium as the carrier gas. The initial mixture was prepared in a 1 L glass bulb on a glass vacuum line. Dilution in He was typically 1/25 with a total pressure of helium of 150 Torr. Gas was deposited via a stainless steel capillary (2 m in length) with a rate of 3 mmol h^{-1} . The deposition nozzle parameters were 1 mm inner diameter at a distance of 20 mm from the cold substrate. At 30 K, Helium does not condense. Typical ice film thickness was less than 500 nm. The infrared measurements (from 4000 to 500 cm^{-1}) were made in a reflection absorption geometry with an incidence angle of 5° to the surface normal using a Bruker 113v spectrometer. Spectra were recorded at 0.5 or 1 cm^{-1} nominal resolution from co-addition of 100 interferograms. In this configuration, only the optical transversal mode (TO) can be excited as in transmission infrared spectroscopy.

Three different photolysis sources were employed: a Nd:YAG laser from Quantel (YG 781–20C) emitting at 266 nm and operating at 20 Hz with a power of $6 \text{ mJ s}^{-1} \text{ cm}^{-2}$, a xenon lamp (Cunow XC 150 S 150 W), and a 90-W medium-pressure mercury lamp (Philips 93136). Surface temperature increase was less than 5 K, and laser induced desorption appeared negligible.

Results and Discussion

A. Spectroscopic Studies. 1. FTIR Studies of ClNO_2 Thin Films Deposited on Au. Thirty years ago, transmission IR spectra of nitrogen 14 and nitrogen 15 isotopic species of nitryl chloride were reported in solid state at 80 K.¹¹ More recently, FT Raman and transmission infrared spectra with ab initio calculations for solid nitryl chloride at 90 K have been described by Durig et al.¹² A RAIR spectrum at a grazing angle of incidence of a ClNO_2 film deposited at 85 K on a gold substrate was also reported by Sodeau.⁹ Our spectra were in good agreement with transmission IR spectra reported in the literature. As expected, they were different from those of ref 9 where the longitudinal modes were observed rather than transversal modes. Figure 1 shows the IR spectrum of ClNO_2 condensed at 30 K from the gas phase and of the same film after annealing at 50, 70, 80, and 90 K. At 30 K, there are two broad bands at 1648.0 and 1254.4 cm^{-1} , two narrower bands at 1315.0 and 784.5 cm^{-1} and a very weak feature at 652.0 cm^{-1} . The band at 1254.4 cm^{-1} with a full width at half-maximum (fwhm) of 13 cm^{-1} is assigned to the symmetric stretching mode of NO (ν_1). The two bands at 1648.0 cm^{-1} (fwhm = 33 cm^{-1}) and 784.5 cm^{-1} (fwhm

TABLE 1: Vibrational Wavenumbers (cm^{-1}) for IR Band Positions of ClNO_2 in the Solid Phase at 30 and 90 K and for ClNO_2 Diluted in Water Ice at 30, 110, and 160 K

	solid ClNO_2 30 K	solid ClNO_2 90 K	ClNO_2 in water ice 30 K	ClNO_2 in water ice 110 K	ClNO_2 in water ice 160 K
$2\nu_4$	3285.0	3282.3			
		3257.4			
$\nu_4 + 2\nu_6$	2955.2	2947.1			
		2942.0			
$\nu_1 + \nu_4$	2900.0	2890.4 sh			
		2884.6			
$\nu_1 + 2\nu_6$	2558.5	2562.9	2559.6	2556.6	2556.6
		2557.7			
$2\nu_1$	2504.5	2505.5	2508.0	2503.0	2501.8
		2499.1			
ν_4	1648.0	1626.5	1646.7	1661.6	1664.5
$2\nu_6$	1315.0	1318.7	1316.2	1314.1	1312.1
		1315.0			
ν_1 in Fermi resonance	1254.4	1254.1	1260.2	1260.8	1261.1
		1251.0			
ν_2	784.5	802.2	789.4	785.7	780.5
		785.1			
ν_6	652.0	652.0			

= 30 cm^{-1}) are assigned to the asymmetric stretching mode of NO (ν_4) and to the symmetric bending mode ν_2 , respectively. Absorption at 1315.0 cm^{-1} (fwhm = 12 cm^{-1}) is due to the harmonic $2\nu_6$ in Fermi resonance with ν_1 . The weak feature at 652.0 cm^{-1} is due to the ν_6 out-of-plane bend mode. The two other modes ν_3 (ν_s^{ClN}) and ν_5 (δ_{as}) are located outside the range these spectra. When the temperature is raised above 80 K, changes in the band profiles occur as shown in Figure 1. The ν_4 band shifts to lower frequency and narrows dramatically by a factor of 10 while the other bands (except the ν_6 band) split into two components. The sharpness of the bands and the fine structure are an indication of a more crystalline ordering. No ionic form of ClNO_2 was observed. Above 100 K, ClNO_2 sublimates very slowly. Several combinations and overtones bands were also identified between 2500 and 3300 cm^{-1} namely $2\nu_4$ (3285.0 cm^{-1}), $\nu_4 + 2\nu_6$ (2955.2 cm^{-1}), $\nu_1 + \nu_4$ (2900.0 cm^{-1}), $\nu_1 + 2\nu_6$ (2558.5 cm^{-1}), and $2\nu_1$ (2504.5 cm^{-1}). Comparison of the frequencies of the vibrational fundamentals overtones and combination modes for neat solid at 30 and 90 K are given in Table 1 (columns 1 and 2). Assignment is based on that of ref 11. The integrated intensity ratios of the $\nu_1/\nu_2/\nu_4$ modes was found to be 1/0.35/2.3 for both amorphous and crystalline forms.

Kinetic studies of the desorption of thick ClNO_2 multilayers were performed at 102, 104, 106, and 108 K from the measurements of integrated intensity of the ν_4 band versus time at a given temperature. Pure ClNO_2 was deposited near the temperature to be studied, and the film was allowed to equilibrate for some minutes at the studied temperature. Film thickness varied in a range (about 200–500 nm) for which integrated intensities of the absorptions are proportional to the column density of ClNO_2 . The data were adequately described by a zero order expression as shown Figure 2A in which, for presentation, curves have been translated to the same origin. The slope of the curves does not give the absolute rate constant k , which is dependent on the absorption coefficient of ν_4 band. However, variation of $\ln k$ versus reciprocal temperature allows the determination of the binding energy of solid ClNO_2 (ΔH_b) from $k = A \exp(-\Delta H_b/RT)$.^{13,14} As seen in Figure 2B, the logarithm of the apparent sublimation rates obtained varies linearly with reciprocal temperature and the enthalpy energy

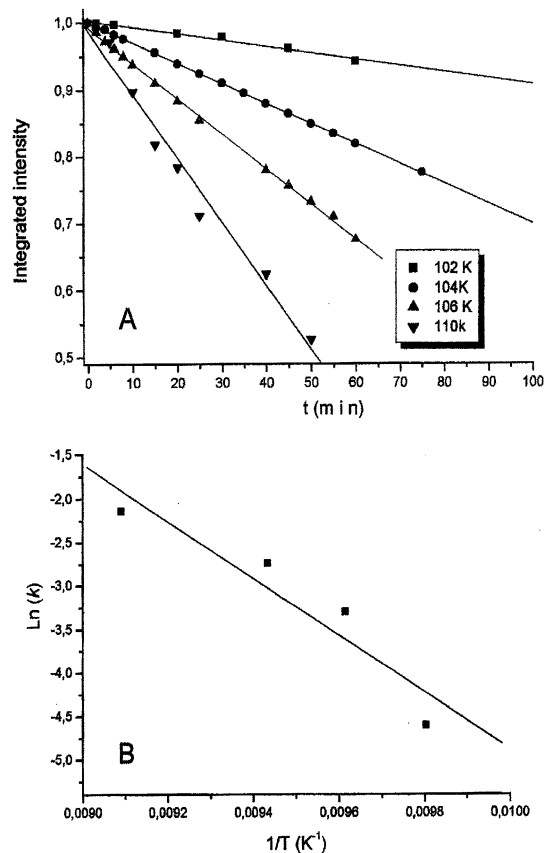


Figure 2. (A) Kinetic curves for pure CINO₂ sublimation at 102, 104, 106, and 110 K. The integrated intensity of the ν_4 CINO₂ absorption is plotted versus time for each temperature. (B) Plots of $\ln(k)$ versus reciprocal temperature. The rate constant k is extracted from the slopes of the curves in Figure 2A.

for sublimation of neat CINO₂ was deduced from the slope of such a plot. We determine ΔH_s to be 32 ± 3 kJ mol⁻¹.

2. *CINO₂ on the Ice Surface.* Water layers deposited as described in the Experimental Section were exposed during different times to a constant pressure of gaseous CINO₂. Exposures of water films to CINO₂ were performed at 30 K on amorphous and crystalline surfaces. Figure 1 shows typical spectra recorded after exposure at 30 K of an amorphous ice

film to CINO₂ during 1 and 3 min. Evolution of the spectrum obtained after 3 min exposure time with temperature is also presented in the Figure 3. As can be seen, the CINO₂ fundamentals are qualitatively similar to the spectrum of pure solid film obtained at this temperature. The only observed change, as shown in Figure 4 with an expanded scale, consists of the appearance, in the ν_{OH} region of water ice, of a very weak absorption at 3678 cm⁻¹ close to the free no hydrogen bonded OH stretch (dangling OH band) located at 3699 cm⁻¹ of unperturbed surface H₂O molecules. The shift of the dangling spectral feature observed upon exposure to CINO₂ corresponds to a perturbation of the dangling OH band at the true surface by the adsorbate. After heating of the film at 70 K, this band began to disappear and another one appeared at 3643 cm⁻¹, resulting probably from trapping of CINO₂ in the micropores of amorphous ice. This trapping was due to the diffusion of CINO₂ above 60 K. In the other spectral regions, no new bands appeared with an increase in temperature. As expected, at 90 K, amorphous CINO₂ multilayers transform into a more crystalline form and start to sublimate above 100 K in concert with the disappearance of the 3643 cm⁻¹ feature. When CINO₂ is totally desorbed, very weak nonstructured bands measured at 1664 , 1312 , and 1250 cm⁻¹ remained. They disappeared totally only at 170 K when water ice sublimated under our basic pressure. They characterize nitril chloride trapped in the bulk. Migration of CINO₂ in the lattice occurs probably above 110 K from hydrogen bonded sites in the pores. Bulk transfer from the surface is probably due to transformation of amorphous ice to crystalline ice which leads to the gradual incorporation of CINO₂ throughout the film from sites associated with lattice defects, grain boundaries, and OH groups. These overall results show that no CINO₂ ionization or dissociation has occurred at the surface or in the bulk. On the amorphous ice surface, CINO₂ is molecularly adsorbed with an orientation leading to a weak hydrogen bond with free water OH oscillators at the surface. In ice pores, the hydrogen bond between CINO₂ and water is reinforced because of cooperative factors created by water molecules surrounding nitril chloride as previously shown for ozone deposited upon the ice surface.¹⁵

The same set of experiments were also performed on a crystalline surface. Cubic ice was formed from water ice deposited at 40 K then slowly annealed at 160 K, or by direct

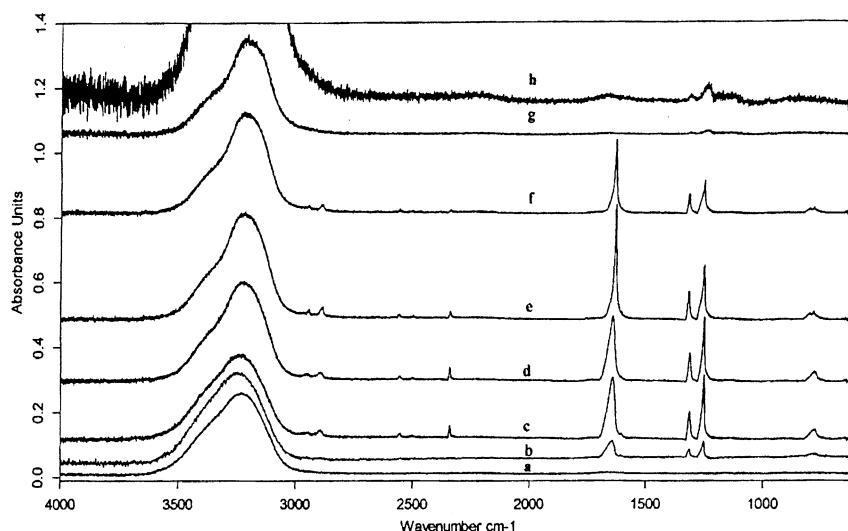


Figure 3. Annealing effects on the spectrum of CINO₂ after deposition at 30 K on a water ice surface: (a) spectrum of ice at 30 K before exposure to CINO₂, (b) after exposure during 1 min to CINO₂ at 30 K, (c) after exposure during 3 min to CINO₂ at 30 K, (d–g) after annealing at 70, 90, 110, and 150 K, respectively. Trace h is the spectrum g after expansion of scale.

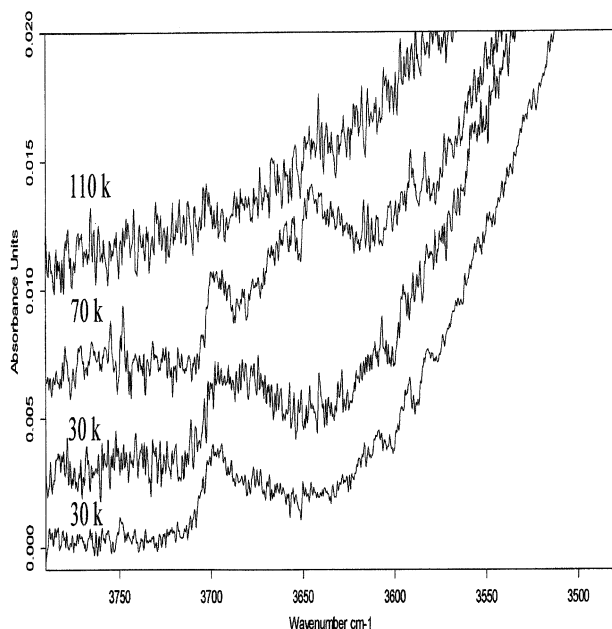


Figure 4. New bands in the dangling OH region appearing in the spectra a, c, d, and f presented in the Figure 3.

deposition of water vapor at 160 K, and then the sample was cooled to 30 K and exposed to CINO₂ vapor. No band at 3678 cm⁻¹ was observed probably because of its weakness. As previously reported, amorphous ice has a high coverage of free OH surface groups compared to the crystalline surface.¹⁶

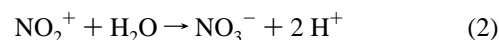
Indeed, absence of CINO₂ ionization on a ice surface below 90 K is not surprising because, at this temperature, the surface is not dynamic and water molecules mobility is inexistent. As a matter of fact, ionization of CINO₂^{17,18} and of covalent N₂O₅^{19,20} on ice surfaces under ultrahigh vacuum was only observed to temperatures above 140 K. Unfortunately, CINO₂ desorbs at 100 K, and other techniques using for example a flow tube reactor are required for investigating CINO₂ uptake on ice surface above 140 K.

3. *CINO₂-Ice Mixtures.* Mixed films of water ice in excess and CINO₂ were prepared by co-depositing CINO₂ and H₂O vapor from two separate inlets onto the gold substrate. Typical initial pressures in each bulb were H₂O/He = 20/150 and CINO₂/He = 4/150. The two gaseous mixtures were deposited via

capillaries with the same rate. Orientation of the two inlets allowed the gas phases to mix just before condensation. After deposition at 30 K, the film was annealed to 200 K at a rate of 3 K min⁻¹, and successive spectra were recorded at different temperatures. Obtained films consisted in a homogeneous diluted solid solution of CINO₂ in water ice. As a matter of fact, the transformation of CINO₂ amorphous phase into crystalline phase was not observed with temperature increase as shown below.

Figure 5 presents a typical result of simultaneous deposition of H₂O and CINO₂ at 30 K and the effect of increase temperature. Only fundamentals of water ice and CINO₂ are observed. No new bands appear between 30 and 170 K indicating that the CINO₂ molecule retains its symmetry in the water matrix environment and that no reaction occurs in this temperature interval. In the ν_{OH} region, a relative intense sharp feature at 3640 cm⁻¹ appears, indicating the formation of a hydrogen bond between CINO₂ and water molecules in the amorphous ice. The vibrational spectrum of CINO₂ diluted in ice is qualitatively comparable to that of amorphous CINO₂. Bands are broad and nonstructured. From 110 to 150K, the profiles and frequencies of CINO₂ absorptions slightly change resulting from the gradual transformation of amorphous ice to cubic ice. Bands became narrower and were shifted either toward the blue (ν₁, ν₄) or toward the red (ν₂). Furthermore, some CINO₂ is released, with the rearrangement of water molecules leading in the opening of some blocked channels. CINO₂ disappears totally at 170 K when water ice begins to sublime. Note that deposition at 160 K of CINO₂ and H₂O gave a spectrum similar to that obtained after annealing at this temperature. Columns 3–5 of the Table 1 compare the frequencies observed at 30, 110, and 160 K.

Thus, solid water ice does not react with CINO₂, whenever in the presence of liquid water CINO₂ dissociates and hydrolyzes via the short-lived intermediate NO₂⁺ according to



Reaction 1 is an equilibrium, and recombination of Cl⁻ and NO₂⁺ could occur in the water matrix cage. However, because of the absence of traces of NO₂⁺ in our spectra, ionization of CINO₂ appears unlikely under our experimental conditions.

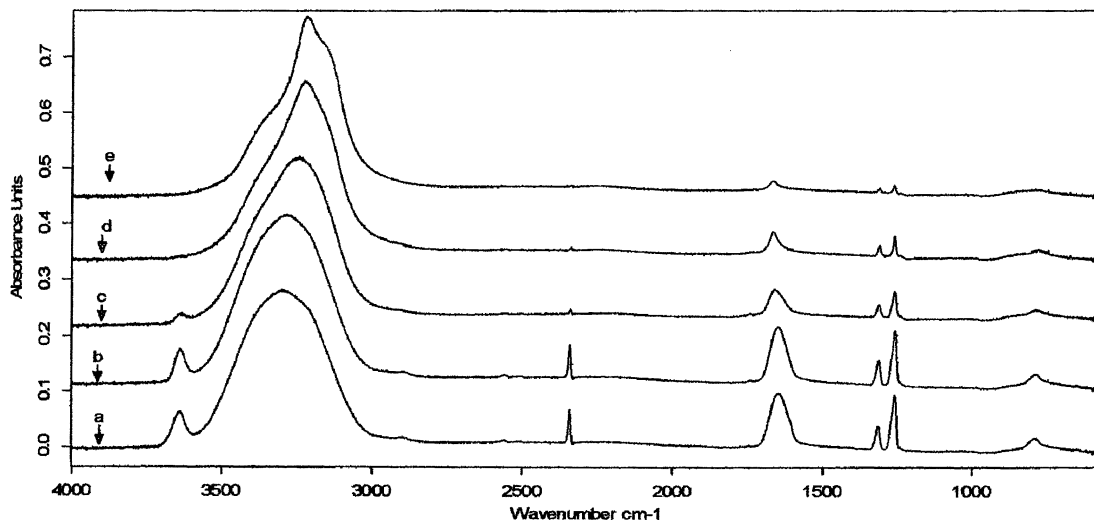


Figure 5. Spectral changes with temperature of a mixed H₂O/CINO₂ film obtained by deposition through two inlets of H₂O/He and CINO₂/He (H₂O/CINO₂ pressure ratio of 10) (a) after deposition at 30 K, (b–e) after annealing at 70, 110, 160, and 165 K, respectively.

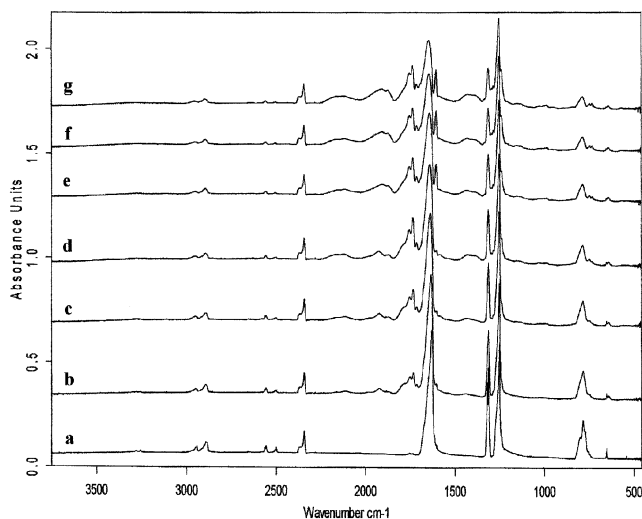


Figure 6. Comparison of the spectra of crystalline ClONO₂ after different irradiation times at 11 K with a 266 nm laser line (photon flux = 8.7×10^{15} photons $\text{cm}^{-2} \text{s}^{-1}$) for 0 (a), 5 (b), 10 (c), 20 (d), 30 (e), 50 (f), and 80 min (g).

Formation of N₂O₄ and ClONO observed by Sodeau et al.⁹ after co-deposition of water and nitryl chloride at 80 K was not confirmed from our experiments and was probably due to an experimental defect.

B. Photochemistry Studies. 1. *The 266 nm Photochemistry of ClONO₂ Thin Films.* Multilayers of crystalline ClONO₂ deposited at 90 K from gaseous ClONO₂ diluted in He were irradiated at 30 K with the 266 nm laser line (photon flux = 8.7×10^{15} photons $\text{cm}^{-2} \text{s}^{-1}$). Figure 6 shows in the 3750–700 cm^{-1} region typical spectra recorded at 30 K after different irradiation times. As can be seen, after exposure of the ClONO₂ film to irradiation, features assigned at ClONO₂ decrease in intensity and new absorptions appear. At the beginning of the irradiation, the main new band which appears is located at 1734.8 cm^{-1} with two shoulders at 1754.1 and 1713.6 cm^{-1} . After 10 min of irradiation, two structured broad bands at 2141 and 1426 cm^{-1} begin to merge, and after 30 min of irradiation, a new absorption only present in trace amounts at the beginning of the irradiation grows and appears as a broad band with two submaxima at 1912 and 1875 cm^{-1} (fwhm = 111 cm^{-1}). In addition, a new narrow absorption appears at 1606 cm^{-1} (fwhm = 10 cm^{-1}). With more

irradiation time (50 min), all of the new bands slowly grow in intensity, and from 50 min of irradiation to more of 120 min, a nearly stationary state is reached. ClONO₂ does not disappear, and it remains at 17% of its initial concentration. Note that under irradiation the profile of crystalline ClONO₂ absorptions change. In contrast to the thin film spectrum after deposition, the spectrum after irradiation does not show any doublet structure, and all bands broaden indicating either an amorphous solid phase under irradiation or formation of ClONO₂ from recombination of photofragments.

Assignment of the bands was not straightforward. However, from comparison of the ClONO₂ spectrum obtained after irradiation with spectra of pure samples of N₂O₄, NO, and ClONO prepared by the deposition of NO₂, NO, and ClONO with helium onto the cold gold foil surface, it was possible to assign the new observed absorptions as illustrated in Figure 7.

The pattern absorption located at about 1734 cm^{-1} can be assigned without ambiguity to N₂O₄ on the basis of the spectrum recorded at 30 K after deposition of a pure NO₂ film. The other characteristic absorption of solid N₂O₄ at 1248 cm^{-1} is overlapped by the ν_1 absorption of ClONO₂. Shoulders at 1754.1 and 1713.6 and the band at 1606 cm^{-1} also observed in the NO₂ film spectrum are due to (NO)₂, N₂O₅, and NO₂, respectively.

From spectra of films obtained by deposition of pure ClONO and pure NO, we assign the band at 1912 cm^{-1} to ClONO and the feature at 1875 cm^{-1} to NO. Bands at 2141 and 1426 cm^{-1} , which exist after deposition of a NO₂ film, grow in concert with an absorption at 1294 cm^{-1} , as shown in Figure 8, when a film of pure NO₂ is irradiated at 266 nm. These bands, which originate from irradiation at 266 nm of solid NO₂, can be assigned to NO⁺ and NO₃⁻. They were observed by Bolduan and Jodl after deposition of NO₂ isolated in a neon matrix at 9 K.²¹ As suggested by Jacox and Thomson, the low frequency of NO⁺ as compared to the frequency of isolated NO⁺ is due to interaction with NO₃⁻.²² Thus, under irradiation, the covalent form of N₂O₄ transforms to an ionic form probably from the asymmetric ONONO₂ isomer identified by the growth of the new band at 1294 cm^{-1} .²³ As observed in nitrogen matrix, under irradiation at 266 nm, sym-N₂O₄ transforms into asym-N₂O₄.³ Irradiation at 266 nm of solid N₂O₄ produces also NO and NO₂ as seen in the Figure 8. From literature data, photolysis of N₂O₄ in the gas phase at 248 nm occurs from two paths, namely, NO₂ + NO₂ and NO₃ + NO.²⁴

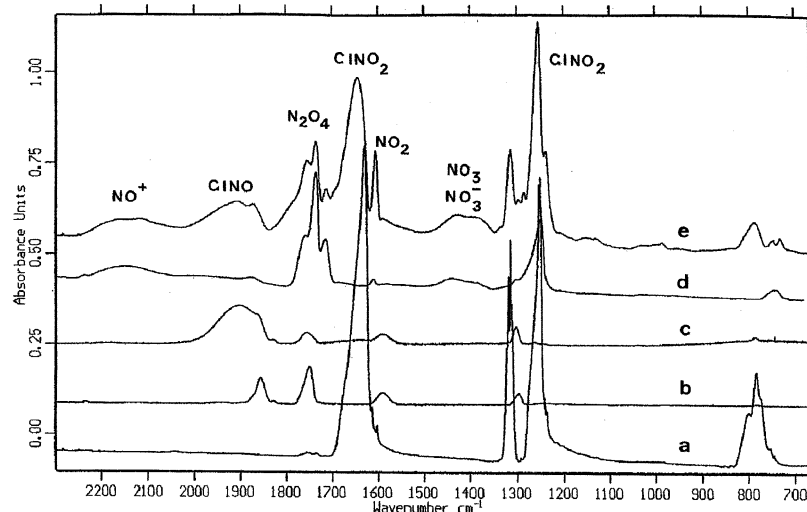


Figure 7. Comparison of the spectrum of a ClONO₂ film after irradiation (trace e) with spectra of films obtained by deposition at 30 K of (b) NO gas, (c) ClONO gas, and (d) NO₂ gas. For comparison, trace a shows the spectrum of e film recorded before irradiation.

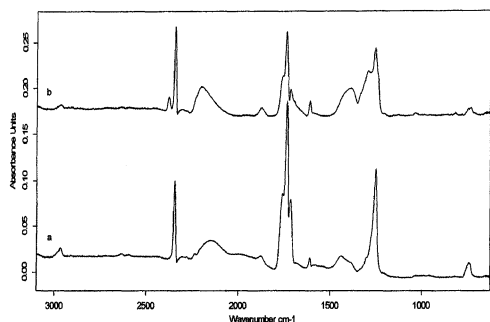
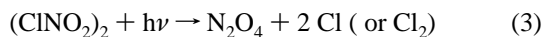


Figure 8. Spectrum evolution of a N_2O_4 film after irradiation at 266 nm (a) after deposition at 30 K of a gaseous NO_2/He mixture, (b) after irradiation.

From the evolution of band intensity described above, it appears that N_2O_4 is the primary product of the photolytic process. Thus, as in the gas phase, the predominant pathway is the photodissociation to NO_2 and Cl . However, in the solid phase, because of clustering of ClNO_2 , N_2O_4 is produced instead of NO_2



This result suggests a primitive unit containing at least two ClNO_2 molecules.

Other observed products which appear after a longer irradiation time only after a significant amount of N_2O_4 is produced (ClNO , NO , NO_2 , NO^+ , NO_3^- , N_2O_5 , and ONONO_2) are due to subsequent secondary reactions. Some possible reactions can be suggested. Indeed, the photolysis of $(\text{ClNO}_2)_2$ results in the production of atomic chlorine which, if it does not produce molecular chlorine, is free to migrate and to react either with N_2O_4 to produce ClNO and NO_3 (for which absorption is close to that of NO_3^-) or with parent ClNO_2 molecules to produce $\text{Cl}_2 + \text{NO}_2$.²⁴ ClNO can be also produced from reaction of atomic chlorine with NO or NO_2 ,²⁵ which are both secondary products. As previously reported, irradiation of solid N_2O_4 at 266 nm produces NO_3^- and NO^+ as well as NO_2 , NO , and NO_3 . At last, traces of N_2O_5 can originate from reaction between NO_2 and NO_3 . Most of the above reactions are probably reversible explaining the photochemical equilibrium observed after a long irradiation time and the change in the ClNO_2 band profile in the course of irradiation.

2. The Photochemistry of ClNO_2 Trapped in Excess of Ice at 30 K. Mixed films were obtained at 30 K by co-deposition through two inlets of gaseous mixtures, $\text{H}_2\text{O}/\text{He}$ and ClNO_2/He ($\text{H}_2\text{O}/\text{ClNO}_2$ initial pressure ratio 5) as described in the previous section. They were irradiated with the 266 nm line and also with the xenon and mercury lamps at 11 K. After irradiation, the temperature was gradually increased to 200 K. Similar qualitative results were obtained with the different irradiation sources.

Figure 9A compares typical spectra recorded in the 3800–500 cm^{-1} frequency range after deposition at 30 K (trace a), after irradiation with the mercury lamp for 3 h (trace b), and after annealing at 200 K without additional irradiation (trace c). The spectrum obtained after irradiation is very different when compared to that recorded after irradiation of a pure ClNO_2 film. Bands belonging to N_2O_4 and to secondary products such as NO^+ , ClNO , and N_2O_5 do not appear. After irradiation (trace b), the spectrum reveals two narrow new bands at 1873 and 1610 cm^{-1} due to NO and NO_2 as well bands at 2740, 2235, 1420, 1301, 1205, 1156, 1038, and 986 cm^{-1} . The difference spectrum between those recorded after irradiation and after

TABLE 2: Product Absorptions in cm^{-1} Observed after UV Irradiation of a Mixed $\text{H}_2\text{O}/\text{ClNO}_2$ Film and after Subsequently Annealing at 200 K

after irradiation	after subsequent annealing at 200 K	assignment
3577		$\text{ClOH}?$
3490		hydrated NO_3^-
	3375–3206	NAT
3111		HNO_3
2740	2720	H_3O^+
2235		H_3O^+
1873		NO
	1844	NAT
1745		H_3O^+
1711		HNO_3
	1652	NAT
1610		NO_2
1420		Hydrated NO_3^-
	1380	NAT
1343		Hydrated NO_3^-
1301		HNO_3
1260		H_3O^+
1245		Hydrated NO_3^-
1244		NAT
1205–1156		H_3O^+
1038		Hydrated NO_3^-
986		HNO_3
834		Hydrated NO_3^-
777		HNO_3
	729–701	NAT
639		H_3O^+

deposition made it easier to identify other absorptions as illustrated in Figure 9B. Other new bands are located at 3577, 3490, 3111, 1745–1711, 1343, 1260–1245, 834, 777, and 639 cm^{-1} . These features correspond to the formation of molecular nitric acid and to amorphous and crystalline nitric acid hydrates based on data appearing in the literature. Previous studies have reported the FTIR spectra of various nitric acid/ice films.^{26–28} These spectra have been assigned as amorphous 1:1, 2:1, and 3:1 $\text{H}_2\text{O}:\text{HNO}_3$ solid solutions at low temperature or as crystalline nitric acid mono (NAM), di (NAD), and tri (NAT) hydrates after deposition at 170 K. The crystalline phases were also obtained after annealing at 200 K of amorphous films. IR spectra for crystalline HNO_3 hydrates and amorphous films do not have distinctly different absorptions and frequencies, but rather they vary from one publication to another. Thus, we are unable to uniquely assign the observed absorptions to specific hydrates. Bands at 3490, 1420, 1343, 1260, and 834 cm^{-1} are characteristic of the hydrated nitrate ion, and bands at 2740, 2235, 1745, 1260, 1156, and 639 cm^{-1} are due to a hydrated oxonium ion as summarized in Table 2. The presence of a band at 3111 cm^{-1} , with absorptions at 1711, 1301, 986, and 777 cm^{-1} suggest also the formation of molecular nitric acid. The weak absorption at 3577 cm^{-1} in the $\nu(\text{OH})$ region could indicate the formation of ClOH .²⁹ To verify formation of nitric acid hydrates, the sample was annealed to 200 K after irradiation for observing possible transformation of nitric acid amorphous hydrates into nitric acid crystalline hydrates. As shown in Figure 9A (trace c), when the temperature is raised to 200 K after irradiation, water ice is removed and changes in the spectrum are observed. In particular, new absorptions at 3375, 3206, 2720, 1844, 1652, 1380, 1244, and 729–701 cm^{-1} appear. They can be assigned to the formation of crystalline NAT from ref 28. This behavior confirms the formation of nitric acid hydrates formed through secondary reactions after irradiation.

Thus, even at low temperature, the photoreactivity data presented here indicates that ice plays a role in the photochem-

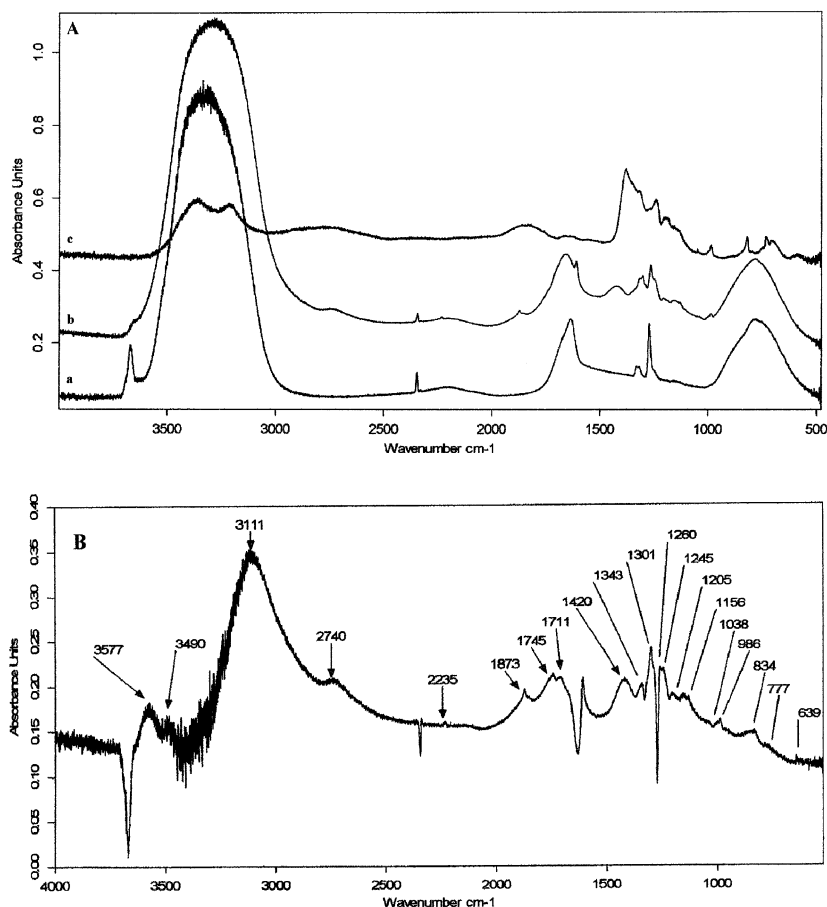
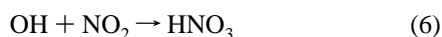
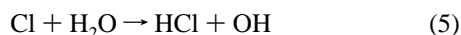
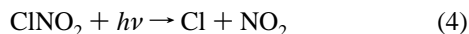


Figure 9. A. Changes in the spectrum of ClONO₂ diluted in amorphous ice after irradiation for 3 h with a mercury lamp and after subsequently annealing at 200 K (a) after deposition at 30 K, (b) after irradiation, (c) after subsequently annealing. B. Difference spectrum of the result of irradiated film shown in Figure 9A (trace b) with film before irradiation (trace a).

istry of ClONO₂ diluted in ice, not for perturbing the nitril chloride's electronic states but rather as a reactive cage leading to secondary products from reaction of water molecules with the primary photo fragments. As in the gas phase or in matrixes, initially, ClONO₂ dissociates probably into Cl and NO₂ then subsequent reactions with water molecules occur. Two possible assumptions can be invoked for the formation of nitric acid hydrates and oxonium ion as final products.

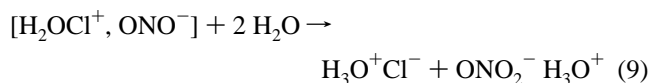
The first possible assumption implies that the two photo-fragments, Cl and NO₂, do not recombine but preferentially react with water molecules. This could be in agreement with the fact that the ClONO₂ molecule which occupies one or two substitutional sites in the ice lattice is surrounded by several molecules of water. Thus, the probability for a reaction of Cl and NO₂ with water molecules is much larger than for the recombination by cage effect of Cl with NO₂. The same behavior was observed after photodissociation of isotopic ozone (O₃¹⁸) trapped at 20 K in a natural oxygen matrix.³⁰ From literature data,³¹ atomic chlorine can react with an adjacent water molecule to form HCl and OH which subsequently can react with NO₂ to produce HNO₃



In water ice, HCl is dissociatively adsorbed to form H₃O⁺Cl⁻ and its hydrate.^{32–33} At large water excess, the molecular nitric

acid formed can ionize to produce hydrated H₃O⁺ and NO₃⁻ ions that we observe. Furthermore, under irradiation, HNO₃ can dissociate into NO and NO₂⁸ also observed in our study.

Another possible assumption involves an ice cage effect. As observed in matrixes,³ the two photofragments, Cl and NO₂, recombine to form the ClONO isomer of nitril chloride which quickly reacts with water molecules to produce the reactive intermediate [H₂O Cl⁺... NO₂⁻] from the nucleophilic attack of the δ⁻ oxygen atom of water molecule on the δ⁺ chlorine atom of ClONO in the same manner than that described for reaction of chlorine nitrate with a water molecule.²⁰ Subsequent hydrolysis of this intermediate can lead to H₃O⁺Cl⁻ and ONO₂⁻ H₃O⁺. The [H₂O Cl⁺] species which can also rapidly hydrolyses to form ClOH and H₃O⁺ was evidenced in the heterogeneous hydrolysis of chlorine nitrate²⁰



Upon irradiation, the nitrate ion, as part of amorphous or crystalline nitric acid hydrates, can produce molecular HONO₂ as shown by T. G. Koch et al.³⁴

Unfortunately, it is not possible with our equipment to chose between these two assumptions and hence to establish accurately the mechanisms.

As mentioned in the Introduction, in the stratosphere, ClNO₂ is produced from reaction of gaseous N₂O₅ with HCl adsorbed on ice. Interestingly, the final photoproducts of ClNO₂ photolysis in amorphous ice are near similar to those observed from hydrolysis of HCl and N₂O₅ on crystalline ice. Indeed at 140 K, exposure of the surface to a saturation amount of HCl results in the formation of amorphous H₃O⁺(H₂O)_nCl⁻³³. Annealing of the covalent N₂O₅ and H₂O mixed film produces nitronium ions, molecular nitric acid, and amorphous nitric acid hydrates²⁰

Conclusions

Interaction of nitryl chloride with water ice between 30 and 180 K and its photochemistry in water amorphous ice as well as in pure solid state have been investigated using single reflection Fourier transform infrared spectroscopy.

On the amorphous ice surface, ClNO₂ is molecularly adsorbed with the formation of a weak hydrogen bond with free water OH oscillators identified by a spectral feature located at 3678 cm⁻¹. Above 60 K, diffusion of ClNO₂ in the ice micropores results in the appearance of a hydrogen bonded OH at 3643 cm⁻¹. With temperature increase, a gradual incorporation of ClNO₂ throughout the film occurs as evidenced by the identification of ClNO₂ trace amounts in the bulk at temperatures above its sublimation temperature.

When ClNO₂ is diluted in the water ice lattice, no reaction is observed even to 160 K. A weak yield of ClNO₂ remains in the lattice till the sublimation of water ice.

Photochemistry at 266 nm of ClNO₂ in ice is different compared to that of pure solid ClNO₂ although the photo dissociation channel leads in both cases to the rupture of Cl and NO₂ as in the gas phase. In the solid, because of clustering, N₂O₄ is observed, whereas in amorphous ice, formation of molecular nitric acid, crystalline nitric acid hydrates, and the hydrated oxonium ion are observed. These products could be formed either by subsequent reactions of Cl and NO₂ photo-fragments with neighboring water molecules of the ice cage or from reaction of ClONO, formed by recombination of Cl and NO₂, with a water molecule.

Although the temperature range investigated in this work is not representative of stratospheric conditions, results reported here can be of some interest for heterogeneous atmospheric chemistry. A large yield of nitryl chloride formed by reaction between N₂O₅ gas with adsorbed HCl on water ice does not react with ice, and consequently, it escapes into the gas phase and decomposes to NO₂ and Cl atoms which contribute to ozone destruction. The small amount remaining in the water lattice leads probably, as in amorphous ice, under irradiation, to similar products to those given by N₂O₅ and HCl in interaction with water ice.

Acknowledgment. This work was performed with financial support from the Program National de Chimie Atmosphérique (PNCA).

References and Notes

- (1) Furlan, A.; Haerberli, M. A.; Robert, H. J. *J. Phys. Chem. A* **2000**, *104*, 10392.
- (2) Nelson, H. H.; Johnston, H. S. *J. Phys. Chem.* **1981**, *85*, 3891.
- (3) Coanga, J. M.; Schriver-Mazzuoli, L.; Schriver, A.; Dahoo, P. R. *Chem. Phys.* **2002**, *276*, 309.
- (4) Behnke, W.; George, C.; Sheer, V.; Zetch, C. *J. Geophys. Res.* **1997**, *102*, 3795.
- (5) Schweitzer, F.; Mirabel, P.; George, C. *J. Phys. Chem. A* **1998**, *102*, 3942.
- (6) Drdla, K.; Turco, R. P.; Elliot, S. J. *Geophys. Res.* **1993**, *98*, 8965.
- (7) Niki, H.; Maker, P. D.; Savage, C. M.; Breitenbach, L. P. *Chem. Phys. Lett.* **1978**, *59*, 78.
- (8) Kawashima, Y.; Takeo, H.; Matsumara, C. *Chem. Phys. Lett.* **1979**, *63*, 119.
- (9) Sodeau, J. R.; Roddis, T. B.; Gane, M. P. *J. Phys. Chem. A* **2000**, *104*, 1890.
- (10) Schmeisser, V. M. Z. *Anorg. Chem.* **1948**, *256*, 33.
- (11) Bernitt, D. L.; Miller, R. H.; Hisatsune, I. C. *Spectrochim. Acta* **1967**, *23A*, 237.
- (12) Durig, J. R.; Hae Kim, Y.; Guirgis, G. A.; McDonald, J. K. *Spectrochim. Acta* **1994**, *50A*, 463.
- (13) Sandford, S. A.; Allamandola, L. J. *Icarus* **1993**, *106*, 478.
- (14) Graham, J. D.; Roberts, J. T.; Brown, L. A.; Vaida, V. *J. Phys. Chem.* **1996**, *100*, 3115.
- (15) Chaabouni, H.; Schriver-Mazzuoli, L.; Schriver, A. *J. Phys. Chem. A* **2000**, *104*, 6962.
- (16) Schaff, J. A.; Roberts, J. T. *J. Phys. Chem.* **1994**, *98*, 6900.
- (17) Sodeau, J. R.; Horn, A. B.; Banham, S. F.; Koch, T. G. *J. Phys. Chem.* **1995**, *99*, 6258.
- (18) Barone, S. B.; Zondlo, M. A.; Tolbert, M. A. *J. Phys. Chem. A* **1997**, *101*, 8643.
- (19) Horn, A. B.; Koch, T. G.; Chester, M. A.; McCoustra, M. R. S.; Sodeau, J. R. *J. Phys. Chem.* **1994**, *98*, 946.
- (20) Koch, T. G.; Banham, S. F.; Sodeau, J. R.; Horn, A. B.; McCoustra, M. R. S.; Chester, A. *J. Geophys. Res.* **1997**, *102*, 1513.
- (21) Bolduan, F.; Jodll, H. *J. Chem. Phys. Lett.* **1981**, *85*, 283.
- (22) Jacox, M. E.; Thomson, W. E. *J. Phys. Chem.* **1990**, *93*, 7609.
- (23) Stirling, A.; Papai, I.; Mink, J.; Salahud, D. R. *J. Phys. Chem.* **1994**, *100*, 2910.
- (24) Watson, R. T. *J. Phys. Chem. Ref. Data* **1977**, *6*, 871.
- (25) Tevault, D. E.; Smardzewski, R. R. *J. Chem. Phys.* **1977**, *67*, 3777.
- (26) Ritzhaupt, G.; Devlin, J. P. *J. Phys. Chem.* **1991**, *95*, 90.
- (27) Smith, R. H.; Leu, M.-T.; Keyser, L. F. *J. Phys. Chem.* **1991**, *95*, 5924.
- (28) Koehler, B. G.; Middlebrook, A.; Tolbert, M. A. *J. Geophys. Res.* **1992**, *97*, 8965.
- (29) Schwager, I.; Arkell, A. *J. Am. Chem. Soc.* **1967**, *89*, 6006.
- (30) Bahou, M.; Schriver-Mazzuoli, L.; Camy-Peyret, C.; Schriver, A. *Chem. Phys. Lett.* **1997**, *273*, 31.
- (31) De More, W. B.; Sander, S. P.; Golden, D. M.; Hamson, R. F.; Kurylo, M. J.; Howard, C. J.; Ravishankara, A.; Kolb, C. B.; Molina, M. J. J. P. L. Chemical kinetics and photochemical data for use in stratospheric modelling. *J.P.L. Publication* **1997**, *12*.
- (32) McCoustra, M. R. S.; Horn, A. B. *Chem. Soc. Rev.* **1994**, *23*, 195.
- (33) Barone, S. B.; Zondlo, M. A.; Tolbert, M. A. *J. Phys. Chem. A* **1999**, *103*, 9717.
- (34) Koch, T. G.; Holmes, N. S.; Roddis, T. B.; Sodeau, J. R. *J. Phys. Chem.* **1996**, *100*, 11402.